

Durability of Reinforced Concrete Containing Biochar and Recycled Polymers

Federica Zanutto^{1,a*}, Alice Sirico^{2,b}, Sebastiano Merchiori^{3,c},
Francesca Vecchi^{2,d}, Andrea Balbo^{1,3,e}, Patrizia Bernardi^{2,f}, Beatrice Belletti^{2,g},
Alessio Malcevschi^{4,h}, Vincenzo Grassi^{1,3,i}, Cecilia Monticelli^{1,3,l}

¹Department of Engineering, Corrosion and Metallurgy Study Centre “A. Daccò”, University of Ferrara, Via G. Saragat 4A, 44122, Ferrara, Italy

²CIDEA & Department of Engineering and Architecture, University of Parma, Parco Area delle Scienze, 181/A, 43124 Parma, Italy

³TekneHub Laboratory, Department of Architecture, University of Ferrara, Via G. Saragat 13, 44122, Ferrara, Italy

⁴CIDEA & Department of Chemistry, Life Sciences and Environmental Sustainability, University of Parma, Parco Area delle Scienze, 11/A, 43124 Parma, Italy

^{a,*}federica.zanutto@unife.it, ^balice.sirico@unipr.it, ^csebastiano.merchiori@unife.it,

^dfrancesca.vecchi@unipr.it, ^eandrea.balbo@unife.it, ^fpatrizia.bernardi@unipr.it,

^gbeatrice.belletti@unipr.it, ^halessio.malcevschi@unipr.it, ⁱvincenzo.grassi@unife.it,

^lcecilia.monticelli@unife.it

Keywords: Recycled aggregates, sustainable concrete, plastic aggregates, biochar, waste

Abstract. In the field of sustainable construction materials, the production of eco-friendly concretes, obtained by the addition of waste products such as biochar and recycled polymer particles, offers interesting alternatives to traditional materials. Biochar is a carbonaceous solid by-product obtained from the thermo-chemical conversion of biomass and its addition into concrete admixtures can offer an eco-friendly carbon sequestration solution, capable to slightly improve concrete properties. Recycled polymer materials can be used to partially replace conventional aggregates with the aim of obtaining lighter concretes that help to face the disposal challenge presented by this non-degradable plastic waste. However, the influence of these waste additions on the corrosion behavior of steel rebars embedded in these “eco-concretes” is still unexplored. Within this context, this work presents some results of an extensive study dealing with the concrete mechanical and physical properties and the rebar corrosion resistance during cyclic exposures to chloride-containing solutions.

Introduction

Concrete is nowadays the most used man-made material on earth and its demand is even increasing, especially in developing countries. More than 20 billion tons are produced each year worldwide and this leads to a high impact on the environment, in terms of both carbon dioxide (CO₂) emissions and consumption of natural resources. For this reason, improving the sustainability of concrete production is an important challenge to face, in order to guarantee the future sustainability of the building industry [1].

One strategy to reduce CO₂ emissions is the adoption of carbon capture and storage technologies, such as the incorporation in the concrete admixture of carbon negative materials. One example of these is biochar, a waste material that is nowadays commonly used as soil amendment or, more generally, in the agriculture-related sector, but it is also often disposed into landfills as a waste, especially when its physical and chemical properties are not in line with agriculture regulations. Biochar represents indeed the solid by-product of thermo-chemical conversion processes, such as pyrolysis and gasification, which transform biomasses into high-value products, such as bio-oil or syngas. However, the valuable physical and chemical properties of biochar and its effectiveness as carbon dioxide sequestration material make its use inside construction materials very attractive. This could lead to environmental benefits, not only in terms of waste management, but also as a strategy

for storing carbon in a stable form in buildings, thanks to the biochar ability to fix a large fraction of stable carbon in its structure. Moreover, the use of biochar in cementitious mixtures can lead to an improvement not only in terms of physical properties, such as thermal and acoustic behavior, shrinkage resistance, water absorption [2-4], but also in terms of mechanical strengths [5-7].

On the other hand, approximately 70% to 85% by mass of concrete is made up of aggregates; hence, their consumption as well as the exploitation of quarries represent problems of maximum severity. A significant reduction in the amount of natural aggregates needed for concrete production can be obtained by using waste products to replace sand and gravel. Among different kind of waste materials, the incorporation of plastics into concrete admixture represents a smart strategy from the point of view of sustainability. Hundreds of million tonnes of plastic waste are produced worldwide, the disposal of which causes a massive negative impact on the ecosystem. Plastics are usually not biodegradable, with polluting effects lasting decades. Hence, recycling them to produce eco-friendly building materials, such as the cementitious ones, appears one of the best solutions for disposing this kind of waste, due to the huge quantities produced annually in terms of both plastics and concretes. For this reason, extensive research studies on the use of plastic waste in concrete can be found [8,9].

The corrosion behavior of steel rebars embedded in concrete containing plastic aggregates or biochar additions and exposed to chloride-containing environments is a very important aspect but to the best of our knowledge, research studies on this topic are still lacking. A few papers describe the effect of plastic aggregates or biochar addition on some concrete properties. Dust plastic particles are reported to improve the resistance of the concrete structure to the aggressive environments and to capillary water penetration, while plastic flakes improve abrasion resistance [10]. Other papers present results in contraraddiction, as they conclude that due to mix difficulties of fresh concrete matrix with recycled plastic particles, the water absorption and the porosity of cured concretes increase so favouring chloride penetration and presumably rebar corrosion [11]. Below 10% addition the increase in water absorption was not observed [12]. In general, plastic aggregates are found to reduce the density and the mechanical properties of concrete [9]. This is attributed to the low plastic particle-cement paste bond strength and the restrained cement hydration reaction near the particle surface resulting from the plastic hydrophobic nature.

The addition of biochar in concrete is reported to improve the concrete pore structure, thus potentially leading to enhanced durability. Moreover, biochar is characterized by a water-retention ability: actually it can strongly absorb water so that the addition of pre-soaked biochar particles to the concrete mix determines the slow water release during curing so acting as an internal curing agent [7,13].

Within this context, this work is mainly focused on analyzing the behavior of green concretes that incorporate biochar or plastic waste in terms of their physico-mechanical properties and in terms of the corrosion protection they afford to the steel reinforcements, during cyclic dry-wet exposures to calcium chloride solutions.

Materials

Four concrete mixes were investigated in this study: a control one (named CEM) produced with ordinary concrete, a concrete mix containing water-saturated biochar (named CHAR) and two concrete mixes containing recycled plastic granules, which were added in substitution of 13% or 20% traditional aggregates (named P13 and P20, respectively).

Reference concrete (CEM) was cast by using cement Type II A-LL 42.5 R, calcareous sand (0/4 mm), siliceous gravel (2/8 mm), water and superplasticizer (Mapei Dynamon Xtend W202R) in the proportions of Table 1.

Biochar was added as a filler, at 5% by weight of cement. The biochar particles used in this work represent the solid by-product of a downdraft fixed-bed pyro-gassificator that uses woodchips of locally-sourced broadleaf trees as incoming biomass. A detailed description of biochar production as well as its physical and chemical characterization can be found in [14].

Table 1. Mix proportions of batches in kg/m³

| Batch | Water | Cement | Sand | Gravel | Biochar | Plastic | Superplasticizer |
|-------|-------|--------|------|--------|---------|---------|------------------|
| CEM | 204 | 408 | 1126 | 562 | - | - | 3.88 |
| CHAR | 204 | 408 | 1126 | 562 | 20.4 | - | 6.52 |
| P13 | 204 | 408 | 900 | 562 | - | 74 | 1.92 |
| P20 | 204 | 408 | 900 | 449 | - | 111 | 1.47 |

Recycled plastic granules, which were characterized by a roughly cylindrical shape, with a base of 3-4 mm and a height of 1-2 mm, were added in partial substitution of natural aggregates. The plastics used in this work were generally disposed of into landfills, because of their variability in composition, i.e. about half of low density polyethylene (LDPE) and half of polyamide (PA).

As can be seen from Table 1, the superplasticizer dosage was properly modified to obtain for all the admixtures the same consistence level, that is slump class S4, as defined by EN 206:2013 [15]. To balance the loss of flowability due to biochar ability of absorbing water [7,13], 68% more of superplasticizer was added in CHAR samples; while lower quantities were required for P13 and P20, respectively equal to 50% and 62% less than that of control. This effect, related to the hydrophobic nature of plastic granules, has obvious advantages, which include the possibility of obtain good workability with lower water content.

Experimental Program

For each concrete mix, seven cubic samples with an edge length of 150 mm were cast: four of them were used to assess compressive strength under standard curing condition, while the other three to determine the hardened density of the four batches analyzed. As regards the samples devoted to measure of compressive strength under standard curing condition, after demolding they were cured in water until the day of testing. At 28 days, compression tests were performed by using an universal testing machine METROCOM PV P30, which works under load control with a loading rate of 0.5 MPa/s, according to EN 12390-3 [16]. Moreover, given the strong water absorption tendency exhibited by biochar and so its ability to release water during the hardening of cementitious composites [13], three additional cubes were cast and cured in air for both CEM and CHAR mixes so as to compare the compressive strength values after water or air curing conditions. CEM and CHAR specimens cured in air after demolding (dry conditions) were called CEM-D and CHAR-D.

The hardened densities were measured on oven-dried specimens according to EN 12390-7 [17]: the samples were put in a ventilated oven at 105±5 °C and the mass was recorded until the mass change in 24 h was less than 0.2%.

In order to analyze the influence of biochar incorporation or recycled plastic addition on the corrosion behavior of the embedded steel rebars, for each concrete batch cylindrical reinforced and unreinforced specimens were cast, with diameter of 60 mm and height of 110 mm (Fig. 1). The unreinforced samples were employed to investigate the rates of chloride penetration, which were reasonably supposed to be equal to those in the corresponding reinforced samples. For the electrochemical measurements, the embedded 6 mm steel rebar acted as a working electrode (W) and an activated titanium wire (fixed in the proximity of the exposed reinforcement area) acted as a quasi-reference low-impedance electrode (R). A coaxial stainless steel net positioned around the concrete cylinders was used as a conterelectrode (C) (not shown in Figure 1). All rebar surfaces were sandblasted, degreased and then partially covered by epoxy resin in order to leave an exposed surface area of about 1000 mm². The curing treatments for samples used for electrochemical tests and chloride analysis were the same as those adopted for mechanical tests. From the point of view of corrosion behaviour, the preparation of D samples for the CHAR mix aimed at assessing the rebar passivation capability in the absence (CHAR-D) and in the presence (CHAR) of water saturation. CEM-D and CEM were the corresponding reference concrete mixes. At the end of the curing time, the upper and lower surface of reinforced and unreinforced specimens were painted by epoxy, to allow chloride penetration only through the lateral specimen surface.

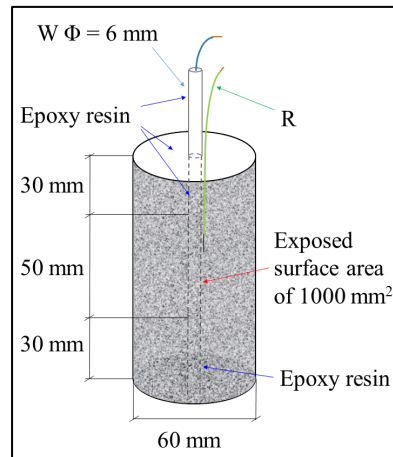


Fig. 1. Details of the specimens for electrochemical measurements

All reinforced and unreinforced specimens were exposed to weekly wet and dry (w/d) cycles in CaCl_2 solution. Each cycle consisted of 4 days of immersion and 3 days of drying under laboratory conditions. The first 12 w/d cycles were performed in 0.2 N CaCl_2 solution, and then in order to accelerate the chloride penetration, the w/d exposure went on in 0.6 N CaCl_2 solution.

Electrochemical tests were performed with a 273A PAR instrument, at the end of the wet step of each w/d cycle. The corrosion potential (E_{cor}) values were evaluated both versus the inner quasi-reference electrode and versus an external saturated calomel electrode (SCE). The polarization resistance (R_p) values were determined potentiostatically by applying an anodic polarization of +10 mV vs E_{cor} for 300 s and by dividing this anodic polarization by the stable anodic current finally measured.

After 5 and 12 w/d cycles, the total chloride concentrations (as wt.% vs. binder) were determined according to standard methods [18,19] in concrete pipes with inner and outer diameters of 6 and 25 mm respectively, obtained by coaxial coring of the unreinforced cylindrical specimens.

Results

The mean compressive strengths, R_c , are reported in Table 2, together with the related standard deviations. Generally speaking, by comparing the values of CHAR with those of the reference concrete mix (CEM), it can be observed that biochar leads to a slight improvement of the compressive strength. The effect of addition of recycled plastics on R_c is more remarkable: the values markedly decrease when plastic is added in the concrete mix, as expected. This effect is due to the hydrophobic nature of plastic, together with the lower hardness of this material compared to that of natural aggregates. As can be observed from in Table 2, the increase in compressive strength operated by the addition of biochar particles is more evident in the case of dry curing of specimens. As a matter of fact, CHAR–D exhibits an increase of more than 17% with respect to control (CEM–D). This effect is related to the ability of biochar of retaining part of mixing water and releasing it gradually during concrete curing [13].

Table 2. Average values of compressive strength and related standard deviations

| Sample | R_c [MPa] |
|--------|-------------|
| CEM | 39.58±1.24 |
| CEM–D | 35.17±1.23 |
| CHAR | 40.79±1.22 |
| CHAR–D | 41.27±2.74 |
| P13 | 28.81±0.24 |
| P20 | 21.13±0.75 |

The positive effect of plastic granules can be seen on density values, δ , which are shown in Table 3 for the four batches analyzed. The partial replacement of natural aggregates with recycled plastics, which are characterised by a particle density less than 1000 kg/m^3 , and therefore much lower with respect to sand and gravel, leads to a reduction of the hardened density of concrete. Also the addition of biochar tends to reduce density, but less significantly if compared to plastic waste. This is due to two opposite mechanisms. On one side biochar tends to reduce concrete density, due to the low density and highly porous nature of biochar particles, but on the other side biochar acts as a filler that reduce the porosity and the amount of free water in fresh mixes. Moreover, both biochar and superplasticizer, which was added at higher percentage in the case of CHAR mix, have little de-aerating abilities.

Table 3. Average values of hardened density and related standard deviations

| Sample | $\delta \text{ [kg/m}^3\text{]}$ |
|--------|----------------------------------|
| CEM | 2119 \pm 6 |
| CHAR | 2078 \pm 11 |
| P13 | 1933 \pm 14 |
| P20 | 1834 \pm 3 |

Table 4 reports the average E_{cor} values (V_{SCE}) of the rebars in CEM (CEM and CEM-D) and CHAR (CHAR and CHAR-D) specimens measured during the curing period under both air and water conditions.

Table 4. E_{cor} (V_{SCE}) measured during curing in air and in water

| Specimens | E_{cor} (V_{SCE}) during curing period | | | |
|-----------|--|--------|---------|---------|
| | 1 day | 9 days | 18 days | 26 days |
| CEM | -0.188 | -0.202 | -0.190 | -0.202 |
| CEM-D | -0.157 | -0.140 | -0.127 | -0.120 |
| CHAR | -0.796 | -0.962 | -0.964 | -0.977 |
| CHAR-D | -0.111 | -0.104 | -0.093 | -0.086 |

While the rebars in CEM, CEM-D, and CHAR-D specimens showed E_{cor} values typical of steel passive conditions at all curing times, water cured CHAR presented very negative E_{cor} values since 1 day of curing ($E_{\text{cor}} = -0.796 V_{\text{SCE}}$), which further shifted in the negative direction and finally reached values of $-0.977 V_{\text{SCE}}$, at the end of the curing period. Thus, on the one side the addition of water-saturated biochar in mortars favors the cement hydration, thanks to the physically bound water slowly available for curing [13], on the other side these results suggest that the high water retention of biochar strongly limits oxygen diffusion towards the rebar surface and hinders passivation. In fact, such negative E_{cor} values are usually encountered in anoxic or almost anoxic conditions [20]

Figure 2 collects the average time trends of E_{cor} and R_p obtained on specimens exposed for 84 days in 0.2 N CaCl_2 solution and then in 0.6 N CaCl_2 solution. During the w/d cycles in 0.2 N CaCl_2 , CEM and CEM-D specimens showed average E_{cor} values around $-0.120 V_{\text{SCE}}$ and R_p which gradually increased up to $4 \div 5 \cdot 10^6 \Omega \cdot \text{cm}^2$, evidencing a passive behaviour. In the same period, CHAR-D and P20 specimens presented a similar behaviour, even if the R_p values of CHAR-D were slightly lower on average (R_p around $2.9 \cdot 10^6 \Omega \cdot \text{cm}^2$) than those of the corresponding CEM-D (R_p around $4.3 \cdot 10^6 \Omega \cdot \text{cm}^2$). A different behaviour was evidenced by P13 and particularly by CHAR specimens. The average E_{cor} of P13 started to shift towards more negative values and R_p value decreased towards the end of the 12th w/d cycle. Within the 12th w/d cycle, CHAR specimens apparently do not reach a fully passive state, as shown by our preliminary results reported in [21]. In fact, the average E_{cor} value of these specimens gradually ennobled from about $-0.960 V_{\text{SCE}}$, at the beginning of the exposure, to about $-0.300 V_{\text{SCE}}$ after 20 days of exposure, then remained more or less constant until the end of the exposure period. Meanwhile, the average R_p values never exceeded $8.5 \cdot 10^5 \Omega \cdot \text{cm}^2$. This seems to suggest that the low oxygen amount reaching the rebar surface is insufficient for full passivation so as to determine low but not negligible corrosion rates. However, the peculiar corrosion conditions of the rebars in this concrete mix need further investigations to be properly defined.

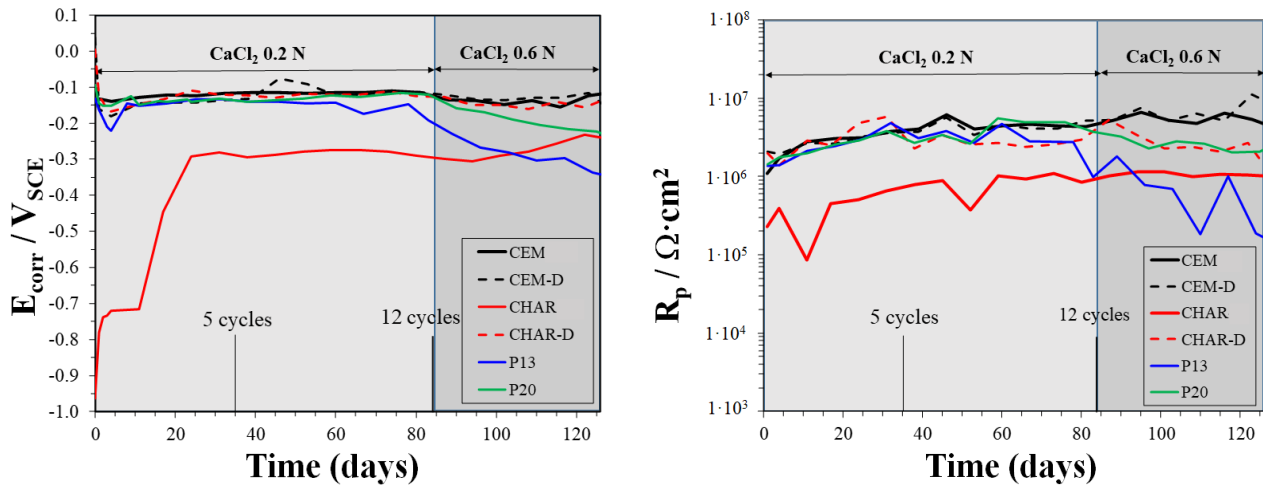


Fig. 2. Time trends of average E_{cor} (left) and R_p (right) values obtained on specimens exposed to weekly w/d cycles in 0.2 N CaCl_2 solution (for 84 days) and then to 0.6 N CaCl_2 solution (until 126 days)

After the 12th w/d cycle, the CaCl_2 concentration was increased to 0.6 N in order to accelerate the chloride penetration and better differentiate the corrosion behavior in the different concrete mixes. CEM, CEM-D, CHAR-D and P20 specimens maintained a stable passive behavior until the end of the investigated monitoring period (126 days - 18 w/d cycles) and CHAR-W specimens retained the previously discussed weak rebar passivity. Instead, P13 evidenced a clear tendency to corrosion propagation: the average E_{cor} shifted continuously in the negative direction and reached a final value of $-0.337 \text{ V}_{\text{SCE}}$, while R_p decreased to $1.9 \cdot 10^5 \Omega \cdot \text{cm}^2$.

The Nyquist plots recorded on the rebars embedded in the different concrete mixes after 12 w/d cycles are shown in Figure 3-left, while Figure 3-right collects the corresponding phase angle vs. frequency plots. The insets in Figure 3-left evidence the high frequency intercepts of the spectra, corresponding to the sum of the pore electrolyte and the concrete resistance between the pseudo-reference Ti electrode and the steel surface (R_{s+c}). This parameter is slightly higher for the plastic containing concretes, likely due to the plastic hydrophobic effect, which hinders the solution penetration.

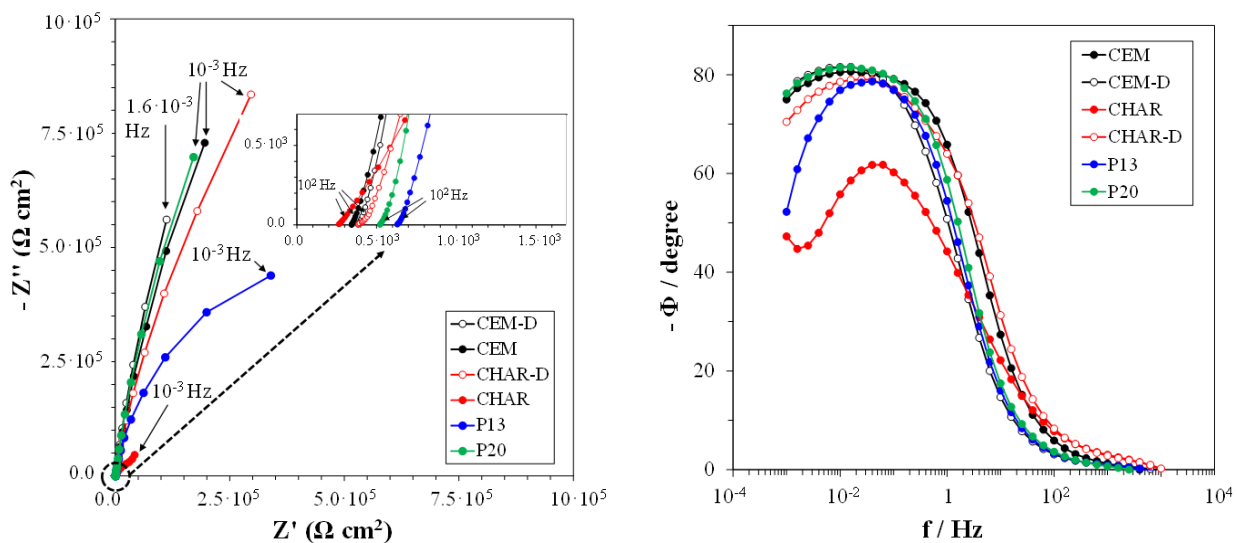


Fig. 3. Nyquist (left) and Bode (phase angle, right) plots obtained after 12 w/d cycles in 0.2 N CaCl_2 solution on steel rebars embedded in the different concrete mixes

At lower frequencies, two capacitive arcs occur in all concrete types: the high frequency one, shown in the inset of Figure 3-left, is scarcely evident and it is likely connected to the dielectric properties of a steel/concrete interface film [22], while the more important low frequency arc is

connected to the corrosion process and can be interpreted by a RC parallel combination linked to the charge transfer resistance and double layer capacitance at the steel surface. P13 and particularly CHAR showed smaller low frequency arc dimensions in agreement with the lower R_p values detected by the potentiostatic method (Figure 2). In the case of CHAR specimens, the low frequency arc was followed by the beginning of a further capacitive arc (as clearly detected in the Bode plot representation of Figure 3-right), likely due to redox reactions in the surface film [20,23]. Table 5 reports the total Cl^- concentrations (as wt. % vs binder) measured after 5 and 12 w/d cycles in the concrete powder fraction closer to the rebar surface (concrete cores with inner and outer diameters of 6 and 25 mm respectively). After 5 w/d cycles, similar total Cl^- concentrations were obtained for both CEM specimens (0.21 % for CEM and 0.23 % for CEM-D), while CHAR, CHAR-D and plastic-containing specimens presented slightly lower values, ranging from 0.14 % for P20 and CHAR to 0.18 % for P13 and 0.19 % for CHAR-D. After 12 w/d cycles, the total Cl^- concentrations in CEM and CHAR-D specimens were significantly higher, with D specimens showing chloride contents higher than those in water-cured ones. This was ascribed to the lower cement hydration degree achieved in D concretes. At the same exposure time, chlorides penetration resulted quite low in concrete specimens containing plastics, with total Cl^- contents of 0.21 % for P20 and 0.25 % for P13. This was likely due to the hydrophobic effect of plastic aggregates, which hinders the penetration of the external solution and therefore the chloride access [24]. Other authors connected it to a reduction in concrete microporosity induced by plastic aggregate addition and to a lower consequent capillary suction [12]. By comparing the average E_{cor} and R_p trends of P13 with the corresponding Cl^- amounts measured near to the rebars, it is evident that in P13 samples corrosion was detected at about 12 w/d cycles, corresponding to a total Cl^- concentration of 0.25 %. These short-term results suggest the development of a weaker passivity on steel rebars in P13, compared to that in CEM. The reason of it was not yet investigated, but possible causes could be: i) incomplete cement hydration close to the binder-plastic aggregate interface, leading to lower pH values of the concrete electrolyte in contact with the rebar surface and a consequent decrease in the critical chloride concentration for corrosion initiation; ii) reduced adherence at the steel-concrete interface and formation of air trapping voids, where early corrosion initiation may occur [25,26].

Table 5. Total Cl^- content (wt.% vs binder) near to the rebar after 5 and 12 w/d cycles

| Total Cl^- [wt.% vs. binder] | | |
|-----------------------------------|--------------|---------------|
| Concrete powder fraction: 6-25 mm | | |
| Specimens | 5 w/d cycles | 12 w/d cycles |
| CEM- | 0.21 | 0.32 |
| CEM-D | 0.23 | 0.55 |
| CHAR | 0.14 | 0.23 |
| CHAR-D | 0.19 | 0.42 |
| P13 | 0.18 | 0.25 |
| P20 | 0.14 | 0.21 |

Conclusions

- The addition of 5% by weight of cement of biochar into concrete (CHAR samples) leads to an increase of compressive strength respect to control (CEM), especially for dry curing (D).
- The use of plastic grains as partial replacement of aggregates (P13, P20) leads to lower compressive strength respect to CEM. However, the positive effects of the use of plastic wastes into concrete admixtures are represented by reduced densities and a lower amount of superplasticizer required.
- During w/d exposure in $CaCl_2$ solutions (12 w/d cycles in 0.2 N $CaCl_2$, followed by 6 w/d cycles in 0.6 N $CaCl_2$ solution), reinforcements in all CEM specimens, in P20 and in CHAR-D specimens remained passive.
- Rebars in CHAR specimens apparently presented a weaker passivity due to a poor access of oxygen to the bars, which prevented full passivity. However, the peculiar rebar corrosion behaviour in this concrete mix needs further investigations to be fully elucidated.

- P13 specimens evidenced corrosion initiation after about 12 w/d cycles.
- After 12 w/d cycles, the concentration of chlorides close to the rebar surface in CHAR and CEM specimens with the same curing conditions was quite similar. For both concrete mixes, D specimens showed an easier access of chlorides, due to the higher porosity induced by lower cement hydration degrees.
- In samples containing granulated plastics, chloride penetration was lower than in CEM and CHAR specimens, due to the plastic hydrophobicity and perhaps to a lower capillary microporosity in the structure of these concretes.
- In P13 samples, an early corrosion initiation was detected after about 12 w/d cycles. The corresponding critical chloride concentration was as low as 0.25 %.

For future developments, the simultaneous addition of biochar and plastic wastes into concrete admixture seems a promising option. Biochar particles, which are able to soak the water not absorbed by plastic grains, could improve the mechanical and durability properties of concrete containing plastics, especially for dry curing, which is typical of practical applications.

Acknowledgements

This research was carried out in the scope of the IMPRESA project (CUP E81F18000310009) supported by POR-FESR 2014-2020 funds (Call 2018). The Authors gratefully acknowledge Cementirosi SpA, Pizzarotti & C. SpA, Mapei SpA and Ecoplast Srl for providing materials for specimen preparation.

We want to remember Professor Cecilia Monticelli, co-author of this work, who passed away recently. We will never forget the years we worked alongside her and we were able to admire her extraordinary professionalism, competence and willingness.

References

- [1] P. J. Monteiro, S. A. Miller, A. Horvath, Towards sustainable concrete, *Nat. Mater.*, 16 (2017) 698-699.
- [2] D. Cuthbertson, U. Berardi, C. Briens, F. Berruti, F. Biochar from residual biomass as a concrete filler for improved thermal and acoustic properties, *Biomass Bioenerg.*, 120 (2019) 77–83.
- [3] S. Gupta, P. Krishnan, A. Kashani, H.W. Kua, Application of biochar from coconut and wood waste to reduce shrinkage and improve physical properties of silica fume-cement mortar, *Constr. Build. Mater.*, 262 (2020) 120688.
- [4] S. Gupta, H.W. Kua, S. Dai Pang, Biochar-mortar composite: Manufacturing, evaluation of physical properties and economic viability, *Constr. Build. Mater.*, 167 (2018), 874-889.
- [5] M. R. Ahmad, B. Chen, H. Duan, Improvement effect of pyrolyzed agro-food biochar on the properties of magnesium phosphate cement, *Sci. Total Environ.*, 718 (2020) 137422.
- [6] S. Gupta, H.W. Kua, C. Y. Low, Use of biochar as carbon sequestering additive in cement mortar. *Cem. Concr. Compos.*, 87 (2018) 110-129.
- [7] A. Sirico, P. Bernardi, B. Belletti, A. Malcevschi, E. Dalcanale, I. Domenichelli, P. Fornoni, E. Moretti. Mechanical characterization of cement-based materials containing biochar from gasification, *Constr. Build. Mater.*, 246 (2020) 118490.
- [8] N. Saikia, N., J. De Brito. Use of plastic waste as aggregate in cement mortar and concrete preparation: A review. *Constr. Build. Mater.*, 34 (2012) 385–401.
- [9] L. Gu, T. Ozbakkaloglu. Use of recycled plastics in concrete: A critical review. *Waste Management*, 51 (2016) 19–42.
- [10] R. Novotny, J. Sal, M. Ctibor, Environmental use of waste materials as admixtures in concrete, 2019 IOP Conf. Ser.: Mater. Sci. Eng. 603 052101.

-
- [11] A.J. Babafemi, B. Šavija, S.C. Paul, V. Anggraini, Engineering Properties of Concrete with Waste Recycled Plastic: A Review, *Sustainability* 2018, 10, 3875.
- [12] B. Coppola, L. Courard, F. Michel, L. Incarnato, P. Scarfato, L. Di Maio, Hygro-thermal and durability properties of a lightweight mortar made with foamed plastic waste aggregates, *Constr. Build. Mater.* 170 (2018) 200–206.
- [13] S. Gupta, H. Wei Kua, Effect of water entrainment by pre-soaked biochar particles on strength and permeability of cement mortar, *Constr. Build. Mater.*, 159 (2018) 107–25.
- [14] A. Sirico, P. Bernardi, C. Sciancalepore, F. Vecchi, A. Malcevschi, B. Belletti, D. Milanese. Biochar from wood waste as additive for structural concrete, *Constr. Build. Mater.* 303 (2021), 124500.
- [15] EN 206:2013+A2:2021. Concrete - Specification, performance, production and conformity
- [16] EN 12390-3:2019. Testing hardened concrete - Part 3: Compressive strength of test specimens
- [17] UNI EN 12390-7:2019. Testing hardened concrete - Part 7: Density of hardened concrete
- [18] ASTM C114, Standard Test Methods for Chemical Analysis of Hydraulic Cement. 2011.
- [19] ASTM C1218 / C1218M – 20, Standard Test Method for Water-Soluble Chloride in Mortar and Concrete. 2020.
- [20] C. Andrade, M. Keddari, X.R. Nóvoa, M.C. Pérez, C.M. Rangel, H. Takenouti, Electrochemical behaviour of steel rebars in concrete: influence of environmental factors and cement chemistry, *Electrochim. Acta* 46 (2001) 3905– 3912
- [21] F. Zanotto, A. Sirico, F. Vecchi, A. Balbo, P. Bernardi, B. Belletti, A. Macevschi, V. Grassi, S. Merchiori, C. Monticelli, Durability of reinforced concrete containing biochar, In: *Proceedings of the fib CACRCS DAYS 2020, on-line event* (2020), 65–72.
- [22] P. Gu, S. Elliot, J.J. Beaudoin, B. Arsenaault, Corrosion resistance of stainless steel in chloride contaminated concrete, *Cem. Concr. Res.* 26 (1996) 1151–1156.
- [23] K. Videm, Phenomena disturbing electrochemical corrosion rate measurements for steel in alkaline environments, *Electrochimica Acta* 46 (2001) 3895– 3903.
- [24] A. Cotto-Ramos, S. Davila, W. Torres-Garcia, A. Caceres-Fernandez, Experimental design of concrete mixtures using recycled plastic, fly ash and silica nanoparticles, *Constr. Build. Mater.* 254 (2020) 119207.
- [25] U.M. Angst, M.R. Geiker, A. Michel, C. Gehlen, H. Wong, O.B. Isgor, B. Elsener, C.M. Hansson, R. François, K. Hornbostel, R. Polder, M. Cruz Alonso, M. Sanchez, M.J. Correia, M. Criado, A. Sagüés, N. Buenfeld, The steel–concrete interface, *Mater. Struct.* 50 (2017) 143.
- [26] U.M. Angst, M.R. Geiker, M. Cruz Alonso, R. Polder, O.B. Isgor, B. Elsener, H. Wong, A. Michel, K. Hornbostel, C. Gehlen, R. François, M. Sanchez, M. Criado, H. Sørensen, C. Hansson, R. Pillai, S. Mundra, J. Gulikers, M. Raupach, J. Pacheco, A. Sagüés, The effect of the steel–concrete interface on chloride-induced corrosion initiation in concrete: a critical review by RILEM TC 262-SCI, *Mater. Struct.* 52 (2019) 88.